5

Modeling the Wake Behind Bluff Bodies for Flow Control at Laminar and Turbulent Reynolds Numbers Using Artificial Neural Networks

Selin Aradag and Akin Paksoy
TOBB University of Economics and Technology, Turkey

1. Introduction

The phenomenon of vortex shedding behind bluff bodies has been a subject of extensive research. Many flows of engineering interest produce this phenomenon and the associated periodic lift and drag response (Cohen et al., 2005). External flow over bluff bodies is an important research area because of its wide range of engineering applications. Although, the geometry of a bluff body can be simple, the flow behind it is chaotic and time-dependent after a certain value of Reynolds number. Forces acting on the body such as drag and lift also vary in time, and cause periodic loading on it. These forces originate from momentum transfer from fluid to the body, where their magnitudes are strongly related to the shape of the body and properties of the flow.

Flow over a circular cylinder is a benchmark problem in literature. It arises in diverse engineering applications such as hydrodynamic loading on marine pipelines, risers, offshore platform support legs, chemical mixing, lift enhancement etc. (Gillies, 1998; Ong et al., 2009). It is experimentally investigated by Norberg (1987) that when the Reynolds number of flow over a circular cylinder exceeds 48, vortices separate from the cylinder surface, and start to move downstream, where steady-state behavior of the flow turns into a time-dependent state. These periodically moving vortices at the downstream form self-excited oscillations called the von Kármán vortex street (Gillies, 1998) as shown in Fig. 1.

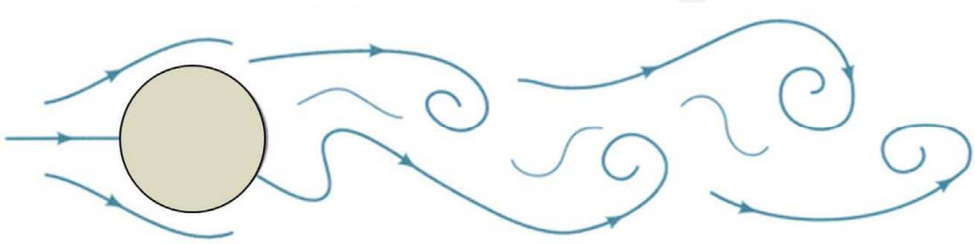

Fig. 1. The von Kármán vortex street observed in the wake region of a two-dimensional circular cylinder

Separation from the surface of the cylinder can be either laminar or turbulent according to the regime of the flow in the boundary layer. It is shown by Wissink and Rodi (2008) that flow with a Reynolds number between 1000 and 20000 is called subcritical, and in this range, boundary layer on the cylinder is entirely laminar and transition from laminar to turbulent flow happens somewhere at the downstream. Although vortex street is fully turbulent after Re≈20000, laminar separation sustains up to a Reynolds number of 100000 (Travin, 1999). Several experimental and computational studies in literature examine the flow over a circular cylinder at subcritical Reynolds numbers (Anderson, 1991; Aradag, 2009; Aradag et al., 2009; Lim and Lee, 2002).

The control of the vortex shedding observed in the wake region of a bluff body is extremely important in engineering applications in order to improve aerodynamic characteristics and performance of the bluff body. To do this, it is substantially important to predict the flow structures and their characteristics observed in the wake region (Aradag, 2009).

In many of the engineering applications involving fluids, Computational Fluid Dynamics (CFD) plays a crucial role as a major tool to analyze flow structures and their characteristics (Gracia, 2010). However, it lacks the functionality of being practical and quick for real-time complex fluid mechanics applications, and such limitations cause difficulties especially in the development of flow control strategies (Fitzpatrick et al., 2005). In order to observe the flow structures and their characteristics in real-time systems in detail, a more practical procedure is needed.

The Proper Orthogonal Decomposition (POD) is a reduced order modeling technique used to analyze experimental and computational data by identifying the most energetic modes and relative mode amplitudes in a sequence of snapshots from a time-dependent system (Cao et al., 2006). It has been used in numerous applications to introduce low-dimensional descriptions of system dynamics by extracting dominant features and trends (Lumley, 1967). The POD technique was originally developed in the context of pattern recognition, and it has been used successfully as a method for determining low-dimensional descriptions for human face, structural vibrations, damage detection and turbulent fluid flows (Chatterjee, 2000). In addition, the method has also been used for many industrial and natural applications, such as supersonic jet modeling, thermal processing of foods, investigation of the dynamic wind pressures acting on buildings, weather forecasting and operational oceanography (Cao et al., 2006). There are several studies in literature that utilize the POD technique in fluid mechanics applications as a reduced order modeling tool (Connell & Kulasiri, 2005; Lieu et al., 2006; O'Donnell & Helenbrook, 2007; Sen et al., 2007; Unal & Rockwell, 2002).

In POD technique, originally correlated data is linearly combined to form principal components that are uncorrelated and ordered according to the portion of the total variance in the considered data (Samarasinghe, 2006). This type of dimensionality reduction offers linear combinations of orthogonal functions to represent a process or a system. Thus, the order of the original high-dimensional data is reduced by compressing the essential information to the uncorrelated principal components associated with modes and relative mode amplitudes to provide a model of the data instead of using the original correlated inputs (Newman, 1996b).

The selected principal components, and hence modes and relative mode amplitudes, can be used as an alternative to the original data ensemble at the input section to a neural network. Since the number of inputs to the model is substantially reduced, the formed network structure will have less complexity and prevent overfitting while representing the original inputs appropriately (Samarasinghe, 2006).

Artificial Neural Networks (ANN's) refer to computing systems the main idea of which is inspired from the analogy of information processing in biological nervous systems. A neural network structure transforms a set of input variables into a set of output variables via mathematical and statistical approaches (Bishop, 1994). By using ANN's, it is possible to obtain a solution for complex problems that do not have an analytical solution via application of conventional approaches.

Currently, neural networks are used for the solution of problems in system identification, such as pattern recognition, data analysis, and control. Apart from these, ANN's have also been applied in diverse fields such as insurance, medicine, economic predictions, speech recognition, image processing, and heat transfer and fluid mechanics applications (Nørgaard et al., 2000). For example, in a study performed by Xie et al. (2009) ANN's are used to evaluate friction factors in shell and tube heat exchangers by making use of experimental and computational Nusselt numbers obtained at laminar and turbulent regimes, where Reynolds number changes within the range of 100 and 10000. The authors related 12 different input sets including geometric parameters, such as number of tubes, arrangement of tubes and fin structures, with Nusselt numbers and friction factors to train the feed-forward backpropagation ANN structure and to predict friction factors for similar geometries. They stated the success of the practical use, easiness and importance of ANN's by achieving only 4% difference between the original data and predicted values.

In another study accomplished by Zhang et al. (1996), ANN's are used to estimate flow characteristics by making use of previously obtained flow dynamics characteristics. The authors observed two-dimensional (2D) von Kármán vortex structures in an elongated rectangular cross-sectional area of a static prism where Reynolds number varies within 250 and 800. They used von Kármán structural phases observed at certain Reynolds numbers as previous cases for prediction of vortex formation phases for new Reynolds numbers. The developed model shows that ANN's provide significant advantages for dealing with flow problems that involve certain amount of complexity to observe flow characteristics without requiring further CFD analyses.

Several notable features of ANN's include relatively high processing speeds, ability of learning the solution of a problem from a set of examples, dealing with imprecise, noisy, and highly complex nonlinear data, and parallel processing (Khataee, 2010). These unique properties make ANN's eligible for prediction of the flow structures and their characteristics in real-time systems for development of flow control strategies.

2. Aims and concerns

The aim of this research is to represent the flow behind a two-dimensional (2D) circular cylinder at laminar and turbulent Reynolds numbers (Re), where Re=100 for the laminar and Re=20000 for the turbulent regime analyses, with the help of Artificial Neural Networks (ANN's) in order to be able to control the vortex shedding formed in the wake region. The flow analyses over the 2D circular cylinder are performed by Computational Fluid Dynamics (CFD), and the results are validated with the experimental results given in literature. In order to observe laminar and turbulent flow structures and their effects in the wake region for control purposes with ANN's, orders of the original CFD data ensembles containing the x-direction velocities at each nodal point of the grids are reduced by application of the Proper Orthogonal Decomposition (POD) technique.

For laminar flow POD analyses, the classical "Snapshot Method" developed by Sirovich (1987) is used; however, for turbulent flows this method causes certain drawbacks, such as lacking the ability of separating flow structures according to their scales during configuration of the modes and relative mode amplitudes. Since it is inevitable to use the POD technique to obtain a low-dimensional description of the original data ensembles for further ANN applications, the classical "Snapshot Method" is combined with the Fast Fourier Transform (FFT) filtering procedure for turbulent flow POD analyses as suggested by Aradag et al (2010). The combined FFT-POD technique is performed to the turbulent CFD data ensembles to eliminate the undesired effects of small scale turbulent structures in the wake region, and to observe flow characteristics in more detail by separating spatial (modes) and temporal (mode amplitudes) structures. (Apacoglu, 2011b)

For real-time flow control applications, it is important to predict the flow based on surface sensors placed at a few discrete points and to relate sensor data as an input to the input section of the neural network structure (Apacoglu et al., 2011a). For this purpose, a sensor placement study is also performed to obtain optimum sensor locations on the 2D circular cylinder surface by using a one-dimensional (1D) classical POD analysis based on surface pressure data of the CFD results. (Apacoglu et al, 2011a)

ANN's are used to predict the temporal structures (mode amplitudes) obtained from the POD and the FFT-POD analyses respectively for laminar and turbulent flow cases by using only the sensor data from several locations on the 2D circular cylinder surface. The training and validation data used for the neural network structure are from several computational cases. Consequently, the defined ANN approach helps to predict what is happening in the flow without requiring further CFD simulations, which are very expensive and impossible in real-time flow control applications. This chapter summarizes the ANN based modeling of the flow structures behind a 2D circular cylinder based on the CFD and POD results given by Apacoglu et al (2011a) for laminar flow and Apacoglu et al (2011b) for turbulent flow. The results obtained in these two articles are used as inputs for training the neural nets in this work.

3. Research methods

3.1 Computational Fluid Dynamics (CFD) methodology

The details on the boundary conditions, grid refinement study and computations are provided in Apacoglu et al. (2011a, 2011b). Operating conditions for the simulations are given in Table 1. The drag coefficient (C_D), Strouhal number (St), pressure coefficient distribution around the cylinder and the velocity profiles at the wake are validated using the experimental results of Lim and Lee (2002), and Aradag (2009).

	Laminar Flow	**Turbulent Flow**	
Parameter	**Value**	**Value**	**Unit**
Reynolds number	100	20000	-
Density	5.25×10^{-5}	0.01056	kg/m^3
Free-Stream Velocity	34	34	m/s
Viscosity	1.78×10^{-5}	1.795×10^{-5}	kg/ms
Pressure	4.337	872.36	Pa

Table 1. Operating conditions for the flow simulations (Apacoglu et al, 2011a, Apacoglu et al, 2011b)

The 2D circular cylinder is designed to comprise four slots on its surface to force the flow by air blowing as shown in Fig. 2. (Apacoglu et al, 2011a)

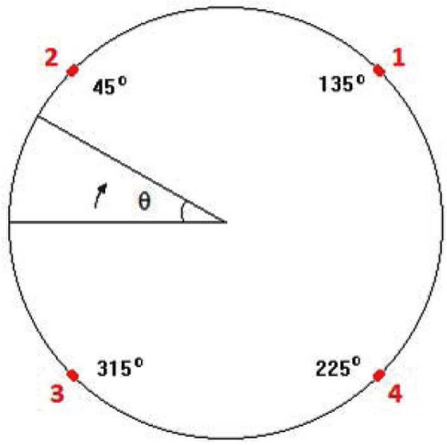

Fig. 2. Position of the slots located on the circumference of the cylinder (Apacoglu et al, 2011a)

Slots are either closed or opened in different combinations at different blowing velocities as outlined below:

- Blowing from all slots, u=0.1U
- Blowing from all slots, u=0.5U
- Blowing from slot numbered 1, u=0.1U
- Blowing from slots numbered 1 and 2, u=0.1U
- Blowing from slots numbered 1 and 4, u=0.1U
- Blowing from slots numbered 2 and 3, u=0.1U
- Blowing from slots numbered 1 and 4, u=0.5U (only at turbulent flow regime)

where u represents blowing velocity and the free stream velocity U=34 $m.s^{-1}$. In order to obtain data ensemble required for the POD and FFT-POD applications, and ANN estimations, velocity values obtained for the x-direction at the wake region are recorded in each time step for 10 periods of the flow time. (Apacoglu et al, 2011a, Apacoglu et al, 2011b)

3.2 Proper Orthogonal Decomposition (POD) and filtering methodology

The POD technique is applied to CFD data ensembles containing x-direction velocity magnitudes observed in the wake region of the 2D circular cylinder in either laminar or turbulent regimes as a post processing to tool to reduce the order of the data and prepare them for further ANN applications. (Apacoglu et al, 2011a, Apacoglu et al, 2011b).

The originally correlated CFD data ensembles are processed to form principal components in space (modes) and time (mode amplitudes). Detailed mathematical and theoretical information is given in Newman (1996a and 1996b), Holmes et al. (1996), Ly and Tran (2001), Sanghi and Hasan (2011) and Smith et al. (2005).

3.3 Sensor placement methodology

Since the ultimate aim of this study is to control the von Kármán vortex street observed in the wake region and to estimate the state of the flow with the help of ANN's, a one-

dimensional (1D) classical snapshot-based POD analysis is carried out on static pressure data obtained directly from the cylinder surface to identify optimal sensor locations. Static pressure data coming from the sensors are essential in training and simulation processes of the neural networks for enabling them to make real-time estimations (Apacoglu et al., 2011).

In practical engineering applications, it is not feasible to place and fix sensors in the wake region and to obtain accurate enough data. On the contrary, body-surface mounted sensors are simple, relatively inexpensive and provide reliable data for further analyses (Seidel et al., 2007).

Sensors identified at optimal locations provide static pressure data, which has the highest activity in terms of pressure on the cylinder surface. This case is demonstrated by an example in a study performed by De Noyer (1999). Since one prominent feature of the POD technique is to extract dominant characteristics of the data, utilization of it to static pressure data coming from the cylinder surface enable optimal locations, which are dominant in terms of pressure for sensor placement.

For laminar and turbulent flow sensor placement POD analyses, CFD data providing static pressure signals on the cylinder surface at 360 locations with one-degree increments are used. In the context of sensor placement studies, uncontrolled flow test case (all slots closed) and the most effective controlled flow test case (all slots open with 0.5U air blowing) are considered for both laminar and turbulent regimes. The details of sensor placement for the laminar case is given by Apacoglu et al (2011a).

For 1D POD analyses, laminar flow test cases (uncontrolled and 0.5U air blowing controlled) include 1800 snapshots, whereas uncontrolled and 0.5U blowing controlled turbulent flow test cases include 1337 and 1320 snapshots respectively. Table 2 shows energy contents of the most energetic four and six pressure-based POD modes turbulent flow. Energy content of each mode represents the level of dominant pressure characteristic trends monitored by that mode.

Mode Number	Energy Contents (%)		Mode Number	Energy Contents (%)	
	Uncontrolled Flow	Controlled Flow		Uncontrolled Flow	Controlled Flow
1	92.14	91.50	4	0.46	0.09
2	4.50	5.43	5	0.29	0.02
3	2.53	0.23	6	0.05	0.01
Total (3 Modes)	99.17	97.16	Total (6 Modes)	99.97	97.28

Table 2. Energy contents of the most energetic four pressure-based POD modes for uncontrolled and controlled turbulent flow test cases

Sensor locations correlated to the energetic surface pressure maxima and minima of pressure-based POD modes are given in Table 3 for turbulent flow test case. The locations of the sensors in Table 3 are referenced in terms of the circumferential angle measured from front stagnation point along the clockwise direction.

For practical applications, it is desirable to reduce the amount of sensors required for the real-time estimation of the systems (Seidel et al., 2007). Since the contributions of the most energetic two and three pressure-based POD modes to the total energy content is greater

than others respectively for laminar and turbulent flow test cases, it is concluded that taking into account only those modes for identification of optimal sensor locations is enough.

Mode Number	Sensor Locations (degrees of angle)			
	Uncontrolled Flow		Controlled Flow	
	Θ_1	Θ_2	Θ_1	Θ_2
1	274	87	274	87
2	224	134	52	307
3	213	184	184	134
4	161	197	177	202
5	161	184	196	161
6	188	202	171	188

Table 3. Sensor locations corresponding to the minimum (Θ_1) and maximum (Θ_2) values of the pressure-based POD modes for uncontrolled and controlled turbulent flow test cases

In addition, when Table 3 is examined in detail, it can be observed that sensor locations corresponding to the most energetic pressure-based POD mode are not affected from air blowing with 0.5U from the slots. Optimal sensor locations for turbulent flow test cases are shown in Fig. 3. The sensors corresponding to the first modes (the most energetic ones) target the periodic modes associated with the von Kármán shedding frequency, whereas the sensors related with other modes target the non-periodic POD modes (Seidel et al., 2007).

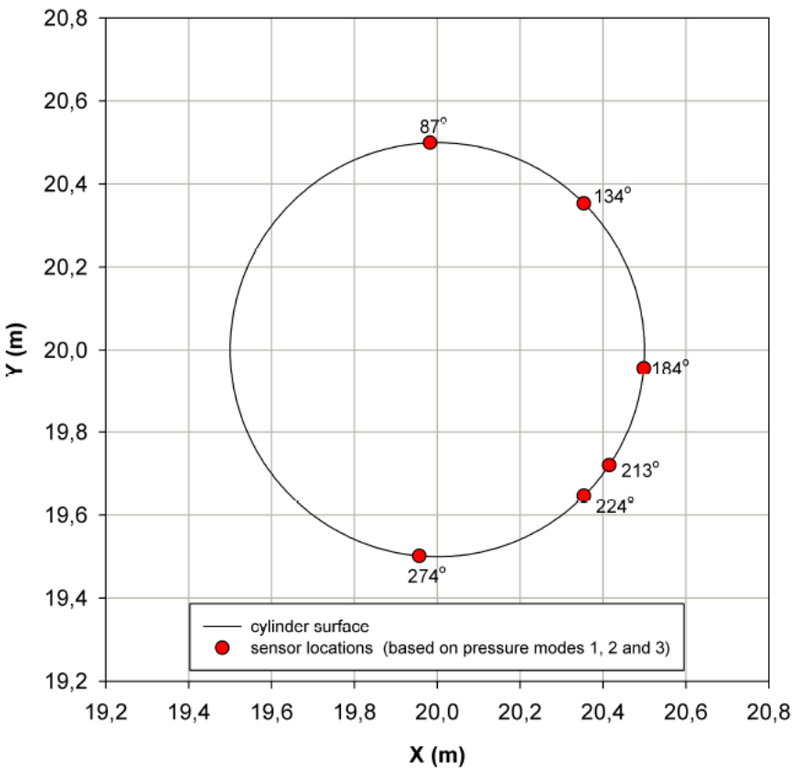

Fig. 3. Optimal sensor locations on the circumference of the cylinder for turbulent flow test cases

3.4 Artificial Neural Network (ANN) methodology

An Artificial Neural Network (ANN) is an interconnected assembly of simple processing elements, the functionality of which is loosely based on the biological neuron. The processing ability of the ANN is stored in the interunit connection strengths, or weights, obtained by a process of adaptation to, or learning from, a set of training patterns (Gurney, 1997).

In ANN, a neuron is a processing element that takes number of inputs, weights them, sums them up, and uses the result as the argument for a singular valued function, which is called the activation function (Nørgaard et al., 2000). Among a variety of network structures the most common one is the multilayer perceptron (MLP) network or also referred as the feedforward network that consists of two or more layers as shown in Fig. 4.

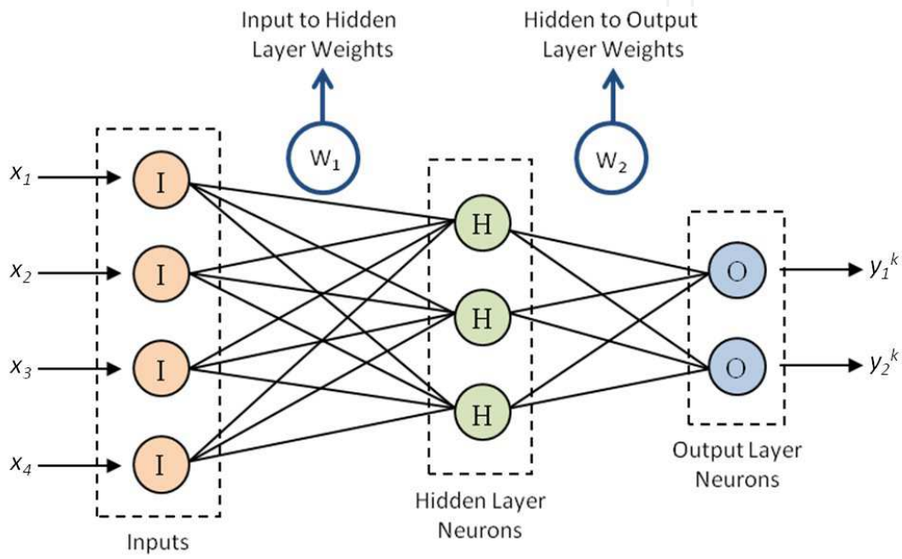

Fig. 4. Schematic representation of the basic structure of an MLP network containing one hidden layer

In Fig. 4, the first layer is known as the hidden layer since it is in some sense hidden between the external inputs (x_1 to x_4) and the output layer, which produces the output of the network (y_{1k} and y_{2k}). W_1 and W_2 are the matrices represent the weight values respectively connecting inputs to hidden layer neurons and correspondingly to output layer neurons. In order to determine the weight values included in W_1 and W_2, there has to be a set of examples of the outputs that are related to the inputs. The determination process of weights from the prior examples is known to be training or learning (Nørgaard et al., 2000; Samarasinghe, 2006).

The MLP neural network structure presents great harmony for discrete-time modeling of nonlinear dynamic systems. Especially turbulent flow systems can be counted as a major example for nonlinear dynamic systems, where the inputs to the network are related to the outputs in a highly nonlinear fashion.

Under some conditions, success of the MLP network structure may be affected negatively from one or more temporal behaviors that the system introduces during identification of the nonlinear relationships and prediction of the time series results by itself. In order to prevent such undesirable drawbacks and to provide accurate enough predictions, the MLP network

structure is supplied with a short-term memory dynamics approach. This kind of neural network structures are called as Spatio-Temporal Time-Lagged Multi Layer Perceptron networks, and they can be thought of as a nonlinear extension of an auto regressive model with exogenous input variables (Samarasinghe, 2006).

In this study, the ANN estimation method of choice including application of the MLP network structure based on a nonlinear system identification in collaboration with Auto-Regressive eXternal input (ARX) model structure approach described by Norgaard et al. (2000) is used. This model includes nonlinear optimization techniques based on the Levenberg-Marquardt back propagation method. The Levenberg-Marquardt method minimizes the difference between the extracted POD mode amplitudes and the ANN estimations, while adjusting the weights of the model.

The Levenberg-Marquardt method is a hybrid algorithm that combines the advantages of the steepest descent and Gauss-Newton methods to produce a more efficient method than either of these two methods does individually. Due to its inherent property related with the conditioning parameter, the Levenberg-Marquardt method adjusts this parameter automatically in every iteration to reduce the error gradually (Samarasinghe, 2006).

The importance of the ARX engaged ANN dynamic network model structure is its strong stability capability even if the dynamic system under investigation is unstable. The stability task is at the highest level of importance when dealing with nonlinear systems of partial differential equations, such as the Navier-Stokes equations (Nørgaard et al., 2000; Siegel et al., 2008).

In this study, pressure data obtained from surface sensors and previously obtained POD or FFT-POD mode amplitudes are used as inputs to the neural network structure. At the end of ANN studies, it is needed to estimate mode amplitudes that are the same as the mode

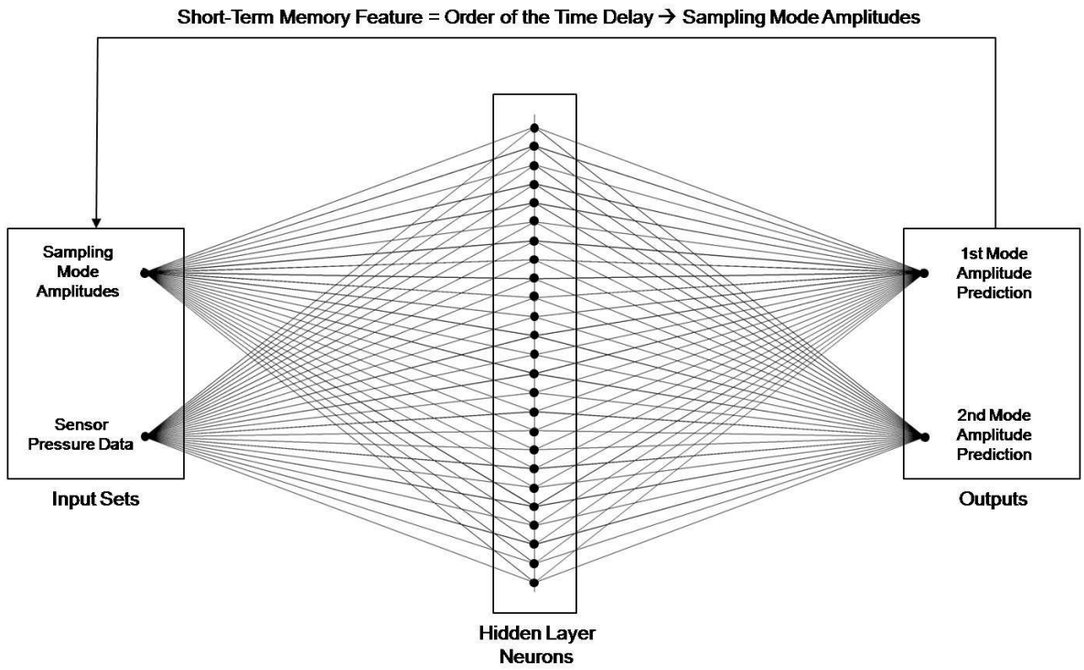

Fig. 5. Schematic representation of the neural network structure formed for analyses

amplitudes obtained from the POD analysis of the CFD results, but without using further CFD simulations. The system consists of multi inputs (sensor pressure data and sampling mode amplitudes coming from short-term memory), and requires multi outputs (each estimated mode amplitude will be an output) as shown in Fig. 5.

Further information about the basics of ANN's, different network structures and applications are given in Haykin (1994), Mehrotra et al. (2000), Samarasinghe (2006), Nørgaard et al. (2000) and Gurney (1997).

4. Results

4.1 Proper Orthogonal Decomposition (POD) and filtering results

The details of the proper orthogonal decomposition analysis are provided in Apacoglu et al (2011a) and Apacoglu et al (2011b)

Figure 6 presents relative FFT-POD mode amplitudes with respect to snapshot number for the uncontrolled (all slots closed) and the most effective controlled flow test case (all slots open with 0.5U air blowing).

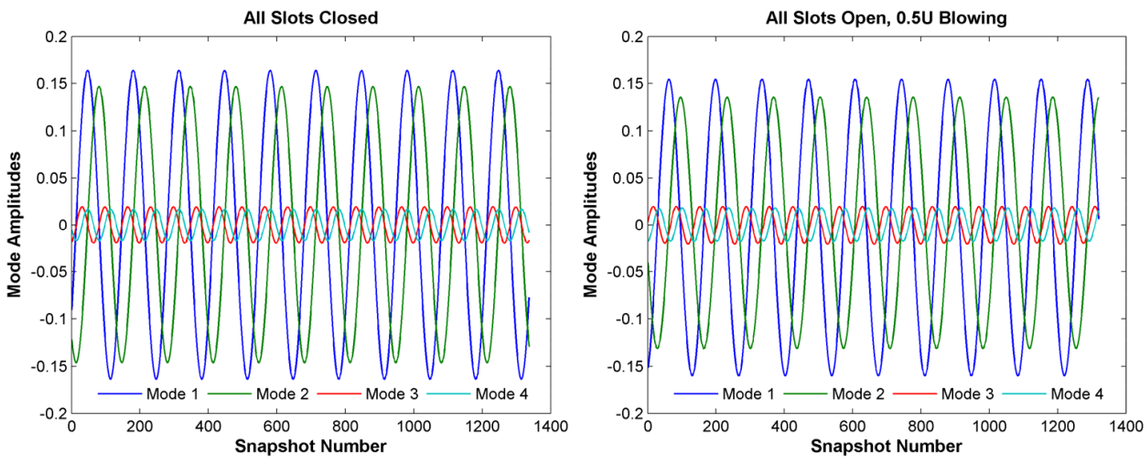

(a) (b)

Fig. 6. Mode amplitudes vs. snapshot number change of the most energetic four FFT-POD modes for a) the uncontrolled (all slots closed) and b) the most effective controlled flow test case (all slots open with 0.5U air blowing)

In Fig. 6, since the most energetic parts of the flow characteristics are related with the modes 1 and 2 in both cases, their amplitudes are greater than modes 3 and 4. All the relative mode amplitudes show periodic behavior, which is directly associated with the existence of the von Kármán vortex street in the wake region of the 2D circular cylinder.

Another important result is that formations of the sinus curves in Fig. 6 are different from each other. For a fixed snapshot number, maximum and minimum values of the mode amplitudes show distinction. This leads to a conclusion that the vortex formation is lagged due to air blowing. By changing air blowing velocity from the slots located on the surface of the cylinder, it is possible that one can bear order of the vortex lagging to desired levels efficiently. More information on mode amplitudes and the results for laminar flow test cases may be found in Apacoglu et al. (2011a) and Paksoy et al. (2010).

4.2 Artificial Neural Network (ANN) results

There are two different Spatio-Temporal Time-Lagged Multi Layer Perceptron networks are formed to be used for laminar and turbulent flow test cases separately. Both network structures are designed to estimate the most energetic two mode amplitudes for different test cases by making use of the specified data sets employed in the training processes.

The generated ANN structures have identical properties. For example, they consist two layers (one hidden and one output) apart from the inputs sections as shown in Fig. 4. The activation neuron function is based on the nonlinear *tanh* function for both networks, and a single bias input has been added to the output from the hidden layer. The output layer has a linear activation function, and it consists of two outputs, namely the most energetic two mode amplitudes.

Both of the designed networks use a supervised learning (training) process with an adequate set of data that constitutes to approximately first half of the 10 shedding cycles. The training process uses cylinder surface pressure data obtained from the six sensors being as one set of the inputs and the sampling mode amplitudes being as the other set of the inputs, which are directly related with the order of the time delay parameter and short-term memory feature of the networks. Thus, the input sections to the networks comprise two different sets of data. After the training process, a validation step is employed by estimating the remaining data (corresponding to last five shedding cycles) to check accuracy and prediction capability of each network.

The complexity and size of the both networks can be adjusted by varying time delay and hidden layer neuron number parameters. The time delay value is directly associated with the order of the short-term memory feature. It qualifies the number of mode amplitudes that

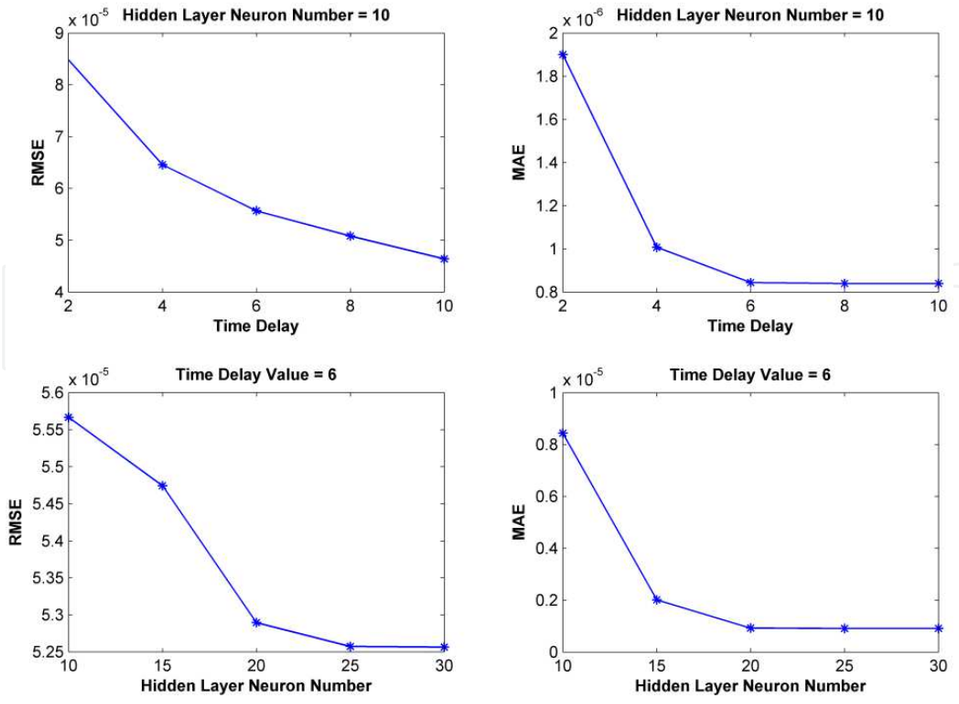

Fig. 7. Performance analysis based on the uncontrolled laminar flow test case

need to be estimated and provided to the inputs section as data observed at the previous sampling instant in addition to the sensor pressure data, which is provided externally to the networks. The hidden layer neuron number is another important parameter that influences prediction accuracy of the estimated mode amplitudes (Paksoy & Aradag, 2011). In order to acquire feasible values for the time delay and the hidden layer neuron number parameters, performances of the networks are monitorized by considering the root mean square errors (RMSE) and mean absolute errors (MAE) between the network prediction results and the target values for a couple of trials. Figures 7 and 8 present network performance analyses based on the uncontrolled flow test cases respectively for laminar and turbulent regimes.

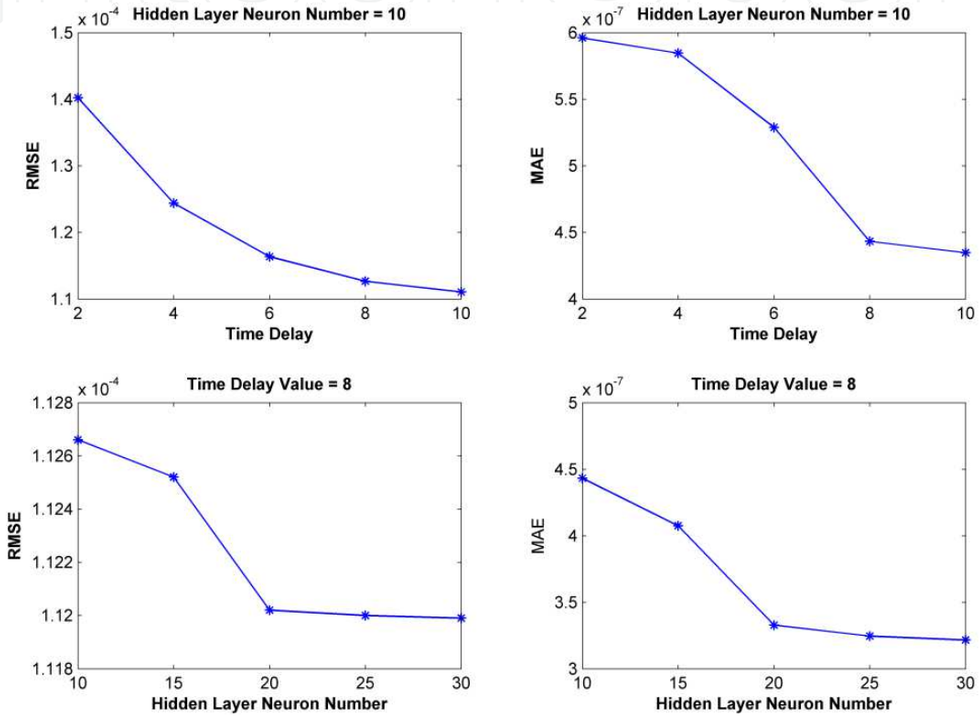

Fig. 8. Performance analysis based on the uncontrolled turbulent flow test case

As shown in Fig. 7 and Fig. 8, an increase in time delay value positively affects accuracy of the results, and relatively decreases the order of the error signals. For larger time delay values, there is more data available for the network to train itself by interconnecting the input sets via setting up larger weighing matrices, and hence weights, by making use of more known data coming from the past. However, this increases complexity of the network structure, and the time required for analyses rises.

According to results observed in Fig. 7 and Fig. 8, values of the time delay and the hidden layer neuron number are respectively specified as 6 and 25 for the laminar flow network structure, 8 and 25 for the turbulent flow network structure.

Taking into consideration of POD (applied for laminar flow test cases) and FFT-POD (applied for turbulent flow test cases) results, it is revealed that more than 90% of the total energy content can be represented by using only the two most energetic modes (1 and 2), where most of the flow structures and their characteristics are retained. For control

purposes, estimations of the mode amplitudes related with those two most energetic modes plays a crucial role in effective observation of the effects flow structures and their characteristics in the flow field without requiring further CFD simulations.

ANN estimations of the mode amplitudes and their comparison with the original data for modes 1 and 2 are shown in Fig. 9 and Fig. 10 so as to observe the convenience of the validation processes for the designed network structures. Uncontrolled flow test cases of both laminar and turbulent flow analyses are selected to be used in the validation process. It can be observed from Fig. 9 and Fig. 10 that the resulting ANN estimations for the validation step show adequate coherency including only minor errors.

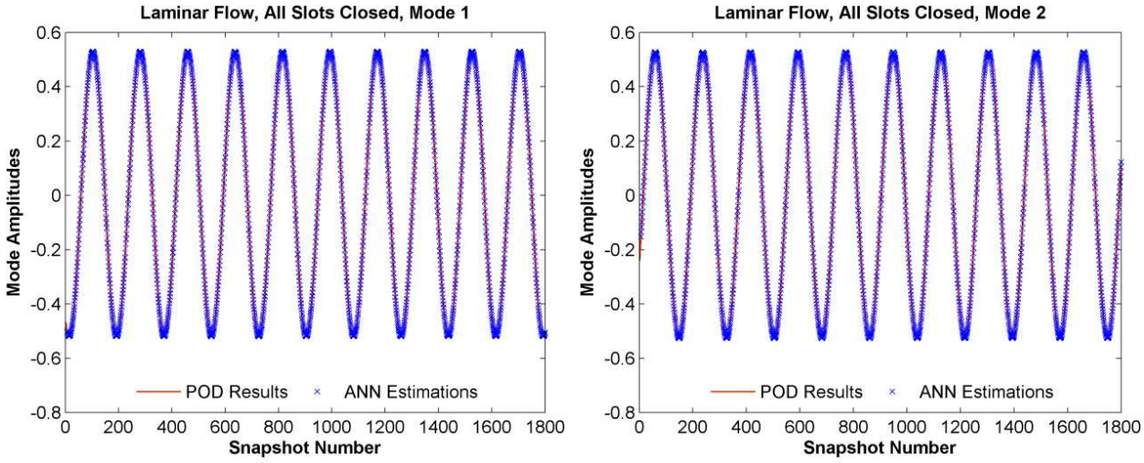

(a) (b)

Fig. 9. Validation process ANN estimations and their comparison with the POD results of the uncontrolled laminar flow test case a) for relative mode amplitude 1 and b) for relative mode amplitude 2 with time delay 6 and hidden layer neuron number 25

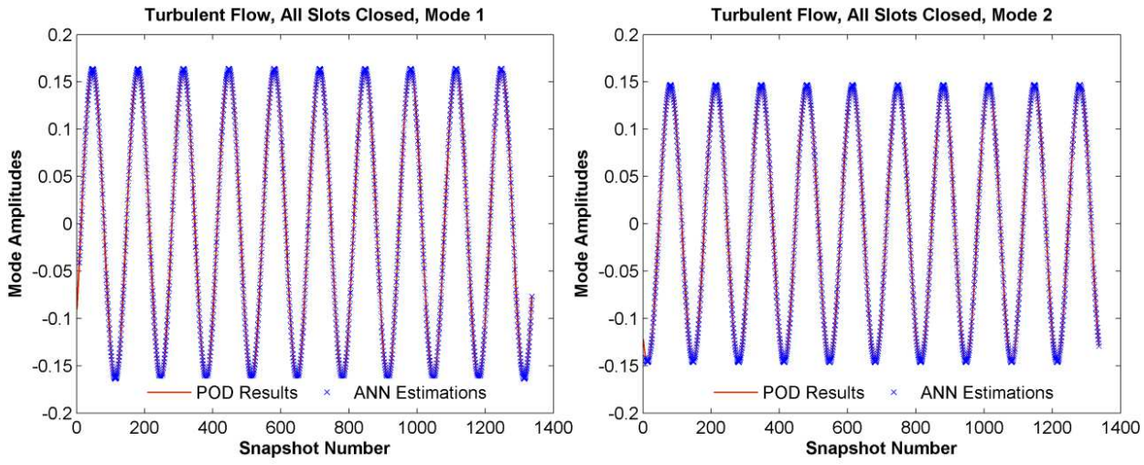

(a) (b)

Fig. 10. Validation process ANN estimations and their comparison with the POD results of the uncontrolled turbulent flow test case a) for relative mode amplitude 1 and b) for relative mode amplitude 2 with time delay 8 and hidden layer neuron number 25

In order to see the modeled network structures in action with the specified design parameters, the networks are adjusted to estimate mode amplitudes for the controlled flow test cases in both laminar and turbulent flow analyses.

For the new estimation cases, different from the validation processes, network structures are trained with the sensor pressure data and sampling mode amplitudes belonging to the all slots open with 0.5U air blowing controlled flow test case for further laminar and turbulent ANN analyses. After training the networks with the specified controlled flow test cases, predictions are done for other controlled flow test cases by just feeding the sensor pressure data regarding to each test case as external input sets.

Figures 11, 12 and 13 show ANN predictions and original mode amplitudes (obtained in the course of POD analyses for laminar flow test cases and FFT-POD analyses for turbulent flow test cases) for a couple of selected sample test cases. Among others, the selected ones exhibit the next most effective control approach with air blowing after the all slots open with 0.5U air blowing controlled flow test case.

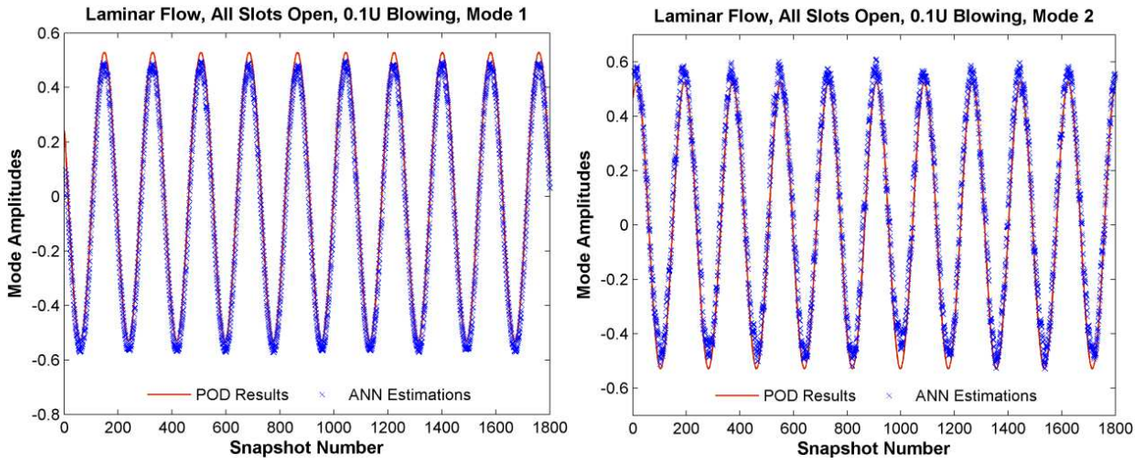

(a) (b)

Fig. 11. ANN results, controlled laminar flow all slots open with 0.1U blowing

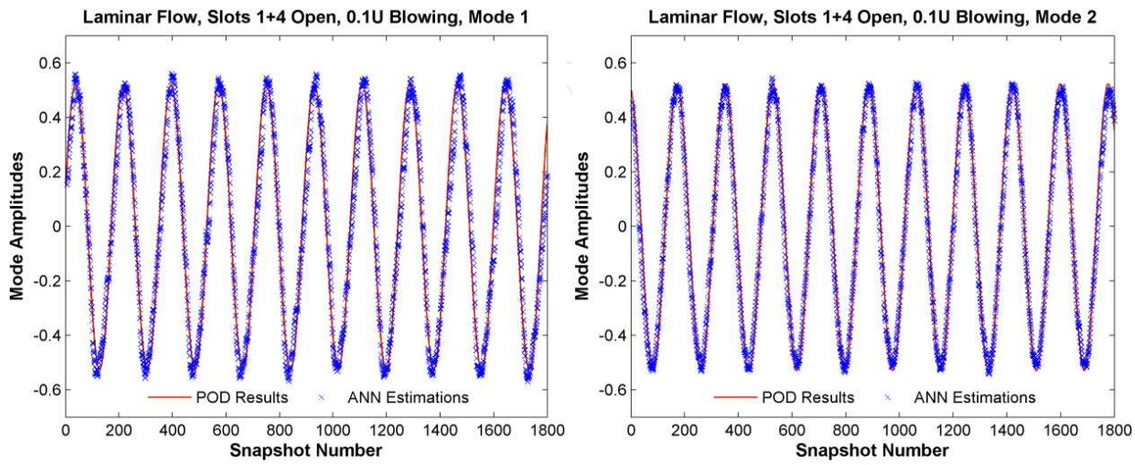

(a) (b)

Fig. 12. ANN results, controlled laminar flow slots 1+4 open with 0.1U air blowing

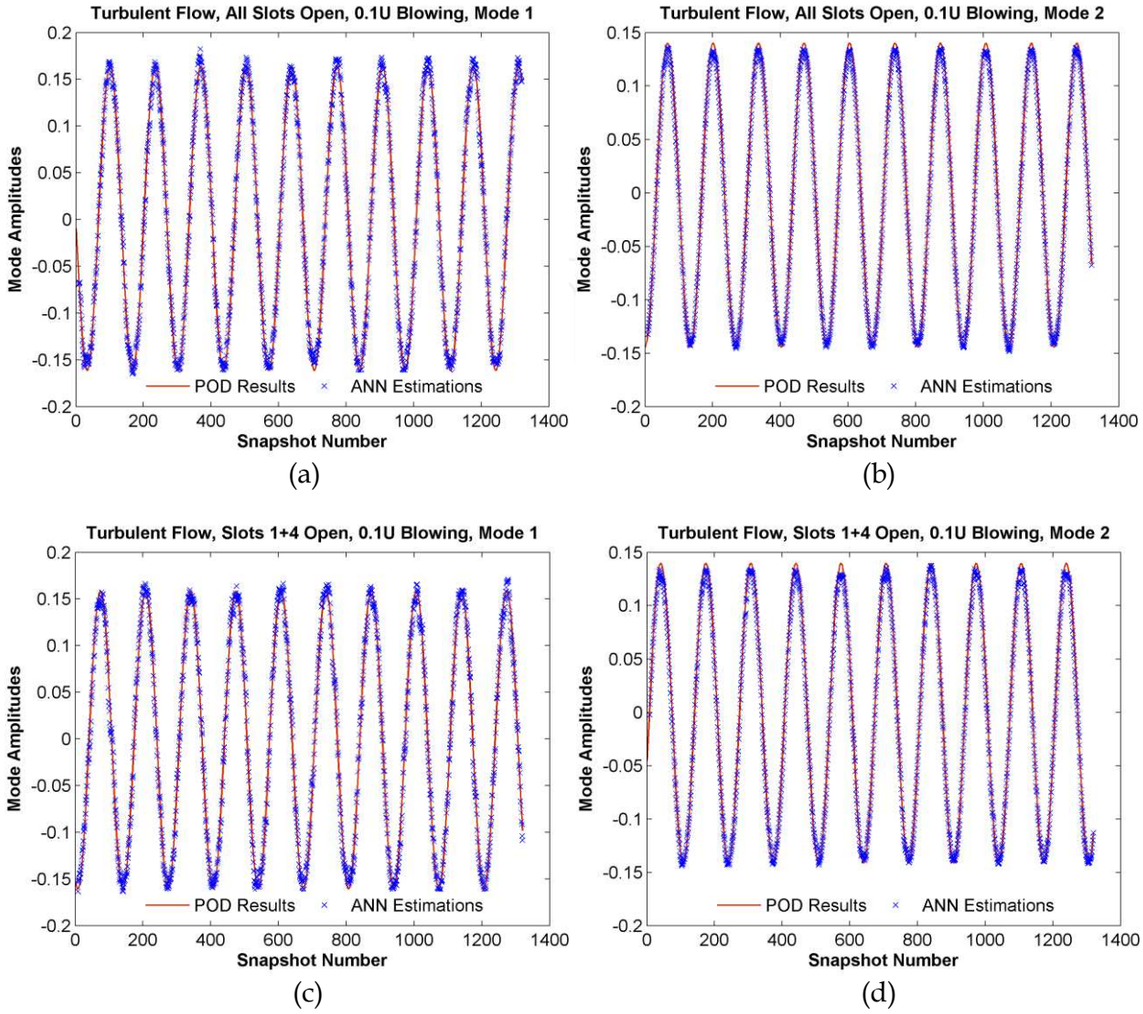

Fig. 13. ANN results, controlled turbulent flow sample test cases

Figures 11, 12 and 13 show that the results obtained from ANN estimations are in good agreement with the results obtained from the POD and the FFT-POD applications. Low-levels of acceptable ANN estimation errors are especially clustered at certain snapshot values corresponding to the lower and upper end tips of the periodic curves.

5. Conclusions

Within the scope of this study, the flow behind a 2D circular cylinder at laminar (Re=100) and turbulent (Re=20000) Reynolds numbers (Re) with the help of Artificial Neural Networks (ANN's) in order to be able to control the vortex shedding formed in the wake region.

For real-time flow control applications, in order to estimate the state of the flow, it is essential to predict the mode amplitudes regarding to the most energetic two modes. ANN's are used to predict mode amplitudes by using only the sensor data from several locations on the 2D circular cylinder surface. By implementation of the Spatio-Temporal Time-Lagged

Multi Layer Perceptron network structures, robust and real-time estimators of mode amplitudes necessary for observation of the effects of flow structures and their characteristics in the flow field are evaluated effectively without requiring further CFD simulations.

6. Acknowledgement

This research is supported by The Scientific and Technological Research Council of Turkey (TUBITAK) under grant 108M549 and Turkish Academy of Sciences Distinguished Young Scientists Awards Programme (TUBA-GEBIP). Major parts of this study were published as a conference proceeding in the 49th AIAA Aerospace Sciences Meeting held in Orlando, Florida in January, 2011.

7. References

Anderson, J.D. (1991). *Fundamentals of Aerodynamics* (2nd Edition), McGraw Hill, New York

Apacoglu, B.; Paksoy, A. & Aradag, S. (2011a). CFD Analysis and Reduced Order Modeling of Uncontrolled and Controlled Laminar Flow over a Circular Cylinder. *Engineering Applications of Computational Fluid Mechanics*, Vol. 5, No. 1, pp. 67-82

Apacoglu, B.; Paksoy, A. & Aradag, S. (2011b), Effects of Air Blowing on Turbulent Flow over a Circular Cylinder, Journal of Thermal Science and Technology, *Journal of Thermal Science and Technology*, in press

Aradag, S. (2009). Unsteady Turbulent Vortex Structure Downstream of a Three Dimensional Cylinder. *Journal of Thermal Science and Technology*, Vol. 29, No. 1, pp. 91-98

Aradag, S.; Cohen, K.; Seaver, C. & McLaughlin, T. (2009). Integrating CFD and Experiments for Undergraduate Research. *Computer Applications in Engineering Education*, doi: 10.1002/cae.20278

Aradag, S.; Siegel, S.; Seidel, J.; Cohen, K. & McLaughlin, T. (2010). Filtered POD-Based Low-Dimensional Modeling of the Three-Dimensional Turbulent Flow Behind a Circular Cylinder. *International Journal for Numerical Methods in Fluids*, doi: 10.1002/fld.2238

Bishop, C.M. (1994). Neural Networks and Their Applications, Review Article. *Review of Scientific Instruments*, Vol. 65, pp. 1803-1832

Cao, Y.; Zhu, J.; Luo, Z. & Navon, I. (2006). Reduced Order Modeling of the Upper Tropical Pacific Ocean Model Using Proper Orthogonal Decomposition. *Computer and Mathematics with Applications*, Vol. 52, No. 8-9, pp. 1373-1386

Chatterjee, A. (2000). *An Introduction to the Proper Orthogonal Decomposition, Computational Science Section Tutorial*. Department of Engineering Science and Mechanics, Penn State University, Pennsylvania

Cohen, K.; Siegel, S.; McLaughlin, T.; Gillies, E. & Myatt, J. (2005). Closed-Loop Approaches to Control of a Wake Flow Modeled by Ginzburg-Landau Equation. *Computers and Fluids*, Vol. 34, pp. 927-949

Connell, R. & Kulasiri, D. (2005). Modeling Velocity Structures in Turbulent Floods Using Proper Orthogonal Decomposition, *Proceedings of International Congress on Modeling and Simulation*, Melbourne, Australia, December 2005

De Noyer, B. (1999). *Tail Buffet Alleviation of High Performance Twin Tail Aircraft using Offset Piezoceramic Stack Actuators and Acceleration Feedback Control*, Ph.D. Thesis, Aerospace Engineering, Georgia Institute of Technology, Atlanta, Georgia

Fitzpatrick, K.; Feng, Y.; Lind R.; Kurdila, A.J. & Mikolaitis, D.W. (2005). Flow Control in a Driven Cavity Incorporating Excitation Phase Differential. *Journal of Guidance, Control and Dynamics*, Vol. 28, pp.63-70

Gillies, E.A. (1998). Low-Dimensional Control of the Circular Cylinder Wake. *Journal of Fluid Mechanics*, Vol. 371, pp. 157-178

Gracia, M.M. (2010). *Reduced Models to Calculate Stationary Solutions for the Lid-Driven Cavity Problem*. M.Sc. Thesis, Department of Aerospace Science and Technology, Universitat Politècnica de Catalunya, Spain

Gurney, K. (1997). *An Introduction to Neural Networks*. CRC Press

Haykin, S. (1994). *Neural Networks*. Macmillan College Printing Company, New Jersey

Holmes, P.; Lumley, J.L. & Berkooz, G. (1996). *Coherent Structures, Dynamical Systems and Symmetry*. Cambridge University Press, Cambridge, UK

Khataee, A.R.; Zarei, M. & Pourhassan, M. (2010). Bioremediation of Malachite Green from Contaminated Water by Three Microalgae: Neural Network Modeling. *Clean-Soil, Air, Water*, Vol. 38, pp. 96-103

Lieu, T.; Farhat, C. & Lesoinne, M. (2006). Reduced-Order Fluid/Structure Modeling of a Complete Aircraft Configuration. *Computer Methods in Applied Mechanics and Engineering*, Vol. 195, No. 41-43, pp. 5730-5742

Lim, H. & Lee, S. (2002). Flow Control of Circular Cylinders with Longitudinal Grooved Surfaces. *AIAA Journal*, Vol. 40, No. 10, pp. 2027-2036

Lumley, J.L. (1967). The Structure of Inhomogeneous Turbulent Flows. *Atmospheric Turbulence and Radio Propagation*, pp.166-178

Ly, H.V. & Tran, H.T. (2001). Modeling and Control of Physical Processes Using Proper Orthogonal Decomposition. *Mathematical and Computer Modeling*, Vol. 33, pp. 223-236

Mehrotra, K.; Chilukuri, K..M. & Ranka, S. (2000). *Elements of Artificial Neural Networks*. The MIT Press

Newman, A.J. (1996a). *Model Reduction via the Karhunen Loéve Expansion Part 1 An Exposition*. Institute for Systems Research, Technical Report No. 96-32

Newman, A.J. (1996b). *Model Reduction via the Karhunen-Loéve Expansion Part 2: Some Elementary Examples*. Institute for Systems Research, Technical Report No. 96-33

Norberg, C. (1987). Effects of Reynolds Number and a Low-Intensity Free Stream Turbulence on the Flow around a Circular Cylinder. Chalmers University of Technology, ISSN 02809265

Nørgaard, M.; Ravin, O.; Poulsen, N.K. & Hansen, L.K. (2000). *Neural Networks for Modeling and Control of Dynamic Systems*. Springer, London

O'Donnell, B. & Helenbrook, B. (2007). *Proper Orthogonal Decomposition and Incompressible Flow: An Application to Particle Modeling*. Computers and Fluids, Vol. 36, No. 7, pp. 1174-1186

Ong, M.C.; Utnes, T.; Holmedal, L.E.; Myrhaug, D. & Pettersen, B. (2009). Numerical Simulation of Flow around a Smooth Circular Cylinder at Very High Reynolds Numbers. *Journal of Marine Structures*, Vol. 22, No. 2, pp. 142-153

Paksoy, A.; Apacoglu, B. & Aradag, S. (2010). Analysis of Flow over a Circular Cylinder by CFD and Reduced Order Modeling, *Proceedings of ASME 10th Biennial Conference on Engineering Systems Design and Analysis*, Istanbul, Turkey, July 2010

Paksoy, A. & Aradag, S. (2011). Prediction of Lid-Driven Cavity Flow Characteristics Using an Artificial Neural Network Based Methodology Combined With CFD and Proper Orthogonal Decomposition, *Proceedings of the 7th International Conference on Computational Heat and Mass Transfer*, Istanbul, Turkey, July 2011

Samarasinghe S. (2006). *Neural Networks for Applied Sciences and Engineering, From Fundamentals to Complex Pattern Recognition*. Auerbach Publications Taylor and Francis Group

Sanghi, S. & Hasan, N. (2011). Proper Orthogonal Decomposition and Its Applications. *Asia-Pacific Journal of Chemical Engineering*, Vol. 6, pp. 120-128

Siegel, S.; Cohen, K.; Seidel, J.; Aradag, S. & McLaughlin, T. (2008). Low Dimensional Model Development Using Double Proper Orthogonal Decomposition and System Identification, *Proceedings of the 4th Flow Control Conference*, Seattle, Washington, June 2008

Seidel, J.; Cohen, K.; Aradag, S.; Siegel, S. & McLaughlin, T. (2007). Reduced Order Modeling of a Turbulent Three Dimensional Cylinder Wake, *Proceedings of the 37th AIAA Fluid Dynamics Conference and Exhibit*, Miami, Florida, June 2007

Sen., M.; Bhaganagar, K. & Juttijudata, V. (2007). Application of Proper Orthogonal Decomposition (POD) to Investigate a Turbulent Boundary Layer in a Channel with Rough Walls. *Journal of Turbulence*, Vol. 8, No. 41

Sirovich, L. (1987). Turbulence and the Dynamics of Coherent Structures, Part I: Coherent Structures. *Quarterly Applied Mathematics*, Vol. 45, No. 3, pp. 561-571

Smith, T.R.; Moehlis, J. & Holmes P. (2005). Low Dimensional Models for Turbulent Plane Couette Flow in a Minimal Flow Unit. *Journal of Fluid Mechanics*, Vol. 538, pp. 71-110.

Travin, A.; Shur, M.; Strelets, M. & Spalart, P. (1999). Detached-Eddy Simulations Past a Circular Cylinder Flow. *Turbulence and Combustion*, Vol. 63, pp. 293- 313

Unal, M. & Rockwell, D. (2002). On Vortex Shedding from a Cylinder, Part 1: The Initial Instability. *Journal of Fluid Mechanics*, Vol. 190, pp. 491-512

Wissink, J.G. & Rodi, W. (2008). Numerical Study of the Near Wake of a Circular Cylinder. *International Journal of Heat and Fluid Flow*, Vol. 29, pp. 1060-1070

Xie G.; Sunden B.; Wang Q. & Tang L. (2009). Performance Predictions of Laminar and Turbulent Heat Transfer and Fluid Flow of Heat Exchangers Having Large TubeRow by Artificial Neural Networks. *International Journal of Heat and Mass Transfer*, Vol. 52, pp. 2484-2497

Zhang, L.; Akiyama, M.; Huang, K.; Sugiyama H. & Ninomiya, N. (1996). Estimation of Flow Patterns by Applying Artificial Neural Networks. *Information Intelligence and Systems*, Vol. 4, pp. 1358-1363

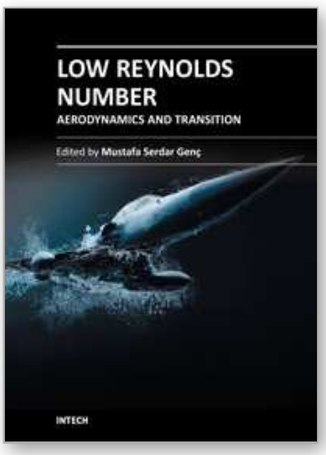

Low Reynolds Number Aerodynamics and Transition

Edited by Dr. Mustafa Serdar Genc

ISBN 978-953-51-0492-6
Hard cover, 162 pages
Publisher InTech
Published online 04, April, 2012
Published in print edition April, 2012

This book reports the latest development and trends in the low Re number aerodynamics, transition from laminar to turbulence, unsteady low Reynolds number flows, experimental studies, numerical transition modelling, control of low Re number flows, and MAV wing aerodynamics. The contributors to each chapter are fluid mechanics and aerodynamics scientists and engineers with strong expertise in their respective fields. As a whole, the studies presented here reveal important new directions toward the realization of applications of MAV and wind turbine blades.

InTech Europe
University Campus STeP Ri
Slavka Krautzeka 83/A
51000 Rijeka, Croatia
Phone: +385 (51) 770 447
Fax: +385 (51) 686 166
www.intechopen.com

InTech China
Unit 405, Office Block, Hotel Equatorial Shanghai
No.65, Yan An Road (West), Shanghai, 200040, China
中国上海市延安西路65号上海国际贵都大饭店办公楼405单元
Phone: +86-21-62489820
Fax: +86-21-62489821

IntechOpen